Article:
Gerassimidou, S, Velis, CA orcid.org/0000-0002-1906-726X and Komilis, D (2020) Establishing a sub-sampling plan for waste-derived solid recovered fuels (SRF): Effects of shredding on representative sample preparation based on theory of sampling (ToS). Waste Management, 113. pp. 430-438. ISSN 0956-053X

https://doi.org/10.1016/j.wasman.2020.06.010

Establishing a sub-sampling plan for waste-derived solid recovered fuels (SRF): Effects of shredding on representative sample preparation based on theory of sampling (ToS)

Spyridoula Gerassimidou[a], Costas A. Velis[a,*], Dimitrios Komilis[b]

[a]School of Civil Engineering, University of Leeds, Leeds, LS2 9JT, United Kingdom

[b]Department of Environmental Engineering, Democritus University of Thrace, Xanthi, Greece

[*]Corresponding author: c.velis@leeds.ac.uk; Telephone: +44 (0) 113 3432327; Room 304, School of Civil Engineering, University of Leeds, Leeds, LS2 9JT, United Kingdom

Declarations of interest: none

Abstract

The uncertainty arising from laboratory sampling (sub-sampling) can compromise the accuracy of analytical results in highly inherent heterogeneous materials, such as solid waste. Here, we aim at advancing our fundamental understanding on the possibility for relatively unbiased, yet affordable and practicable sub-sampling, benefiting from state of the art equipment, theoretical calculations by the theory of sampling (ToS) and implementation of best sub-sampling practices. Solid recovered fuel (SRF) was selected as a case of a solid waste sample with intermediate heterogeneity and chlorine (Cl) as an analyte with intermediate variability amongst waste properties. ToS nomographs were constructed for different sample preparation scenarios presenting the trend of uncertainty during sub-sampling. Nomographs showed that primary shredding (final $d_{90} \leq 0.4$ cm) can reduce the uncertainty 11 times compared to an unshredded final sub-sample ($d \approx 3$ cm), whereas cryogenic shredding in the final sub-sample can decrease the uncertainty more than three times compared to primary shredding (final $d_{90} \leq 0.015$ cm). Practices that can introduce bias during sub-sampling, such as mass loss, moisture loss and insufficient Cl recovery were negligible. Experimental results indicated a substantial possibility to obtain a representative final sub-sample (uncertainty ≤ 15%) with the established sub-sampling plan (57 – 93% with 95% confidence), although this possibility can be considerably improved by drawing two final sub-samples instead (91 – 98% with 95% confidence). The applicability of ToS formula in waste-derived materials has to be investigated as theoretical ToS calculations gave a poorer performance of the sub-sampling plan than experimental results.

Keywords

Resource recovery; Solid recovered fuel (SRF); Sub-sampling; Uncertainty; Theory of sampling (ToS); Shredding

Nomenclature

ANOVA	Analysis of variance
BC	Bomb calorimetry
c	Mineralogical factor
C	Sampling constant
CEN	European Committee of Standardization
Cl	Chlorine
d	Particle size
EC	European Commission
f	Shape factor
FE	Fundamental error
g	Granulometric factor
HDPE	High density polyethylene
IC	Ion chromatography
l	Liberation factor
MT	Mechanical treatment
MC	Moisture content
M_s	Mass of sample
M_L	Mass of lot
MSW	Municipal solid waste
NaCl	Sodium chloride
NIR	Near infrared
PET	Polyethylene terephthalate
PP	Polypropylene
PSD	Particle size distribution
PVC	Polyvinyl chloride
R	Recovery
SRF	Solid recovered fuel
Total [Cl]	Concentration of total chlorine
w/w_d	Weight concentration on dry basis

1. Introduction

Quantifying and harnessing variability remains a major challenge for turning waste materials into secondary resources, and therefore a key barrier to a genuine circular economy (Esbensen and Velis, 2016). Inherent material heterogeneity can introduce significant uncertainty during sampling and laboratory sample preparation, i.e. sub-sampling, and therefore compromises the accuracy of analytical results (Edjabou et al., 2015; Nocerino et al., 2005). Laboratory sub-sampling is the process by which the initially obtained sample is split into sub-samples consecutive times until the generation of a final test sub-sample from which a small mass is drawn for analytical determination, known as test portion (Nocerino et al., 2005; Prichard and Barwick, 2007). Sub-sampling can be designed and executed with a high level of control, with a view to minimise introduction of bias within reason of available resources (time and effort) (Gerlach and Nocerino, 2003). Despite that, design and implementation of optimal sub-sampling plans have received minimal attention to date (Cuperus et al., 2005; Gerlach and Nocerino, 2003).

The relevant theoretical approaches and practical recommendations benefiting from the Theory of Sampling (ToS) (Pitard, 1993) to test sub-sampling variations have received almost no attention. If quantified evidence on the effectiveness of sub-sampling practices existed, optimal cost-effective sub-sampling approaches could be suggested and adopted (Dominy et al., 2018a; Dominy et al., 2018b). ToS addresses the factors that can induce sampling uncertainty and provides practices for its minimization. The fundamental principle of ToS states that "*all fragments in the lot (the entire body from which a sample is drawn) must end up in the final sample with identical and nonzero probability*" (Pitard, 1993). ToS developed a theoretical model for the prediction of the sampling uncertainty resulting from constitutional heterogeneity of material (Gy, 2012). Estimation of theoretical uncertainty due

to sub-sampling can be calculated and depicted as nomographs, enabling the design of optimal sub-sampling plans, associated with a targeted level of tolerable uncertainty (Gerlach and Nocerino, 2003).

The selection of sub-sampling techniques and shredding processes constitute the sub-sampling plan. The performance of a variety of sub-sampling techniques, such as riffle splitting, coning and quartering, fractional shovelling, etc. is described elsewhere (Gerlach et al., 2002; Gerlach and Nocerino, 2003). The beneficial role of shredding in sampling is double: material homogenization creating more uniform and equal probabilities of all particles to be included in the sample; and liberation of analyte which otherwise might be occluded in large particles making difficult to detect it during analysis (Gy, 2012).

However, incorrect practices induced during sub-sampling, such as human mistakes, loss of mass, contamination, chemical modification, physical and biological alteration of the sample (Edjabou et al., 2015; Pitard, 1993), may introduce bias increasing the uncertainty (Edjabou et al., 2015; Nocerino et al., 2005). Shredding can exceptionally induce such practices, albeit the beneficial role it plays in the sampling process. For example, the heat generated during shredding may induce evaporation of a highly volatile analyte, such as mercury (Gerlach and Nocerino, 2003). Insufficient shredding may lead to: i) a systematic error during analytical determination, e.g. incomplete recovery of chlorine (Cl) during bomb calorimetry (BC) (Cuperus et al., 2005); and ii) a wider range of particle size in the sample generating different probabilities of each particle to be included in the test sub-sample (Dominy et al., 2018a). Loss of mass can occur during sub-sampling due to either inappropriate handling of equipment, (e.g. use of riffle splitters by an unskilled operator) or equipment operation (e.g. dropping grains during shredding) (Gerlach and Nocerino, 2003).

The establishment of a sampling and sub-sampling plan able to meet end-users requirements (fitness for purpose) is a critical quality assurance measure (Dominy et al., 2019; Dominy et al., 2018b). For example, waste-to-energy plants need accurately determined quality of the waste-derived material, such as solid recovered fuel (SRF), to ascertain efficient utilization (Flamme and Ceiping, 2014). SRF can contain considerable levels of chlorine (Cl) content, a technical limiting factor for SRF application, due to various chlorinated compounds present in waste items, such as plastic and textiles (Gerassimidou et al., 2020; Iacovidou et al., 2018). This condition in combination with SRF high inherent heterogeneity due to its origin (e.g. MSW (Cheng et al., 2017)), yet lower compared to MSW (Kallassy et al., 2008; Velis et al., 2010), features the importance of representative analytical results (Gerassimidou et al., 2020).

Herein, we aim at advancing our fundamental understanding on the possibility for relatively un-biased, yet affordable and practicable sub-sampling, benefiting from state of the art equipment (e.g. riffle dividers and cryogenic shredding), theoretical calculations by ToS (nomograms) and careful implementation of best sub-sampling practices, with a view to minimize bias. To this, based on an empirically optimal sub-sampling configuration, we: (i) quantify the effects of alternative shredding options on the obtainment of representative test sub-samples based on ToS; (ii) examine the introduction of bias during sub-sampling; (iii) assess the performance of the selected sub-sampling plan according to experimentally derived results; and iv) establish a fitness for purpose sub-sampling plan for solid waste characterization. We demonstrate these for the case of SRF, chosen as a case of solid waste-derived material with intermediate heterogeneity; and for the analyte of total chlorine (Cl), chosen as the one with intermediate variability for solid waste mixtures. Results inform best practice and set the basis for incorporation in relevant sub-sampling standards.

2. Materials and Methods

2.1 Materials

We used a typical SRF sample (ca. 1kg) produced from residual MSW in a mechanical treatment (MT) plant in the UK, processing a mixture of residual household MSW and commercial waste (corporate name withheld for confidentiality reasons). The analytical technique for the determination of total Cl concentration (Total [Cl]) (see **2.2.6**) involved reagents, 0.2 M KOH as absorption solution, Palintest acidifying and silver nitrate tablets (Sigma-Aldrich, UK). Liquid nitrogen was used for the cryogenic shredding. Reference materials (Sigma-Aldrich, UK) were used to resemble SRF composition and calculate the recovery of Cl: powder microcrystalline cellulose, alkali lignin, xylan from beechwood, high density polyethylene (HDPE), isotactic polypropylene (PP), polyethylene terephthalate (PET) and polyvinyl chloride (PVC).

2.2 Methodology

We estimated the sub-sampling uncertainty for different sub-sampling scenarios using state of the art equipment and the ToS formula (see **2.2.2**) to examine the beneficial role of shredding and establish a sub-sampling protocol that fulfils the fitness for purpose requirements. The design of this protocol focused on the development of a straightforward and affordable sub-sampling process suitable for solid waste materials. During the established sub-sampling process relied on practices and equipment proposed by ToS, we monitored incorrect sub-sampling practices to examine the adverse effects of shredding on sub-sampling uncertainty. The selected critical component was Cl, which is the most important technical parameter for SRF applications (BS 15359, 2011). This choice was a compromise between SRF properties with low and high variability amongst waste components, such as moisture

content and mercury, respectively (BS 15442, 2011). In addition, the selected mass of SRF sample (ca. 1kg) approximates the minimum typical sample mass received in the laboratory from the production plant, which can be ranged between 0.8 and 159 kg depending on the grain size and bulk density according to BS 15442 (2011).

2.2.1 Sub-sampling protocol

The sub-sampling process consisted of two stages of shredding and multiple stages of mass splitting according to BS 15413 (2011) (**Figure 1**). The sub-sampling operations and equipment were applied as follows: The SRF sample was pre-dried at 40 ºC for 24 h to remove the moisture that could interfere with the shredding process (BS 15414-3, 2011) (**1**). After pre-drying the sample mass was reduced at 850 g. The pre-dried sample was spread on a canvas forming a thin layer (≤ 2 cm) and a magnet passed over the layer to pick any ferrous metals that could damage the shredders (**2**). The pre-dried sample with a particle size ca. 3 cm was divided into two sub-samples with large riffle splitters (RT 75, Retsch, Germany) (**3**). The sub-samples were shredded with cutting mill (SM 300, Retsch, Germany) to a particle size $d_{90} \leq 4$ mm (primary shredding) (**4**). The shredded sub-samples were divided with small riffle splitters (PFEUFFER GmbH, Germany) multiple times obtaining 16 sub-samples of ca. 50 g each (**5**). A test sub-sample of 7 g was drawn from each of the 16 sub-samples with riffle splitting and cryogenically shredded (Cryomill, Retsch, Germany) to $d_{90} \leq 150$ µm (secondary shredding) (**6**). From these 16 test sub-samples of 7 g, we obtain three test portions for analytical determination of Cl (0.3 g) and moisture content (1 g) as specified by the related CEN standards (see **2.2.2**) (**7**).

Cutting mill is suitable for primary size reduction of highly heterogeneous materials, such as solid waste including soft, medium-hard, elastic and fibrous materials able to achieve a defined final fineness from the first shredding run (Retsch, 2020b). The process is conducted

by the sample comminution between the blades and the stationary double acting cutting bars (Retsch, 2020b). Cryomill is suitable for secondary cryogenic shredding (material feed size ≤ 8mm) producing a fine particle size under inert atmosphere at very low temperature (-196 ºC) through an autofill liquid nitrogen system.(Retsch, 2020a). Cryomill provides programmable shredding conditions depending on the configuration settings and the feed material, which enables to adjust the cost of the process (Retsch, 2011). Cryogenic shredding prevents component evaporation, oxidation and/or microbial degradation due to the integrated cooling system earing interest on sample preparation of solid waste (Junghare et al., 2017). The advantages of cryogenic shredding to sample preparation have been extensively discussed (Junghare et al., 2017).

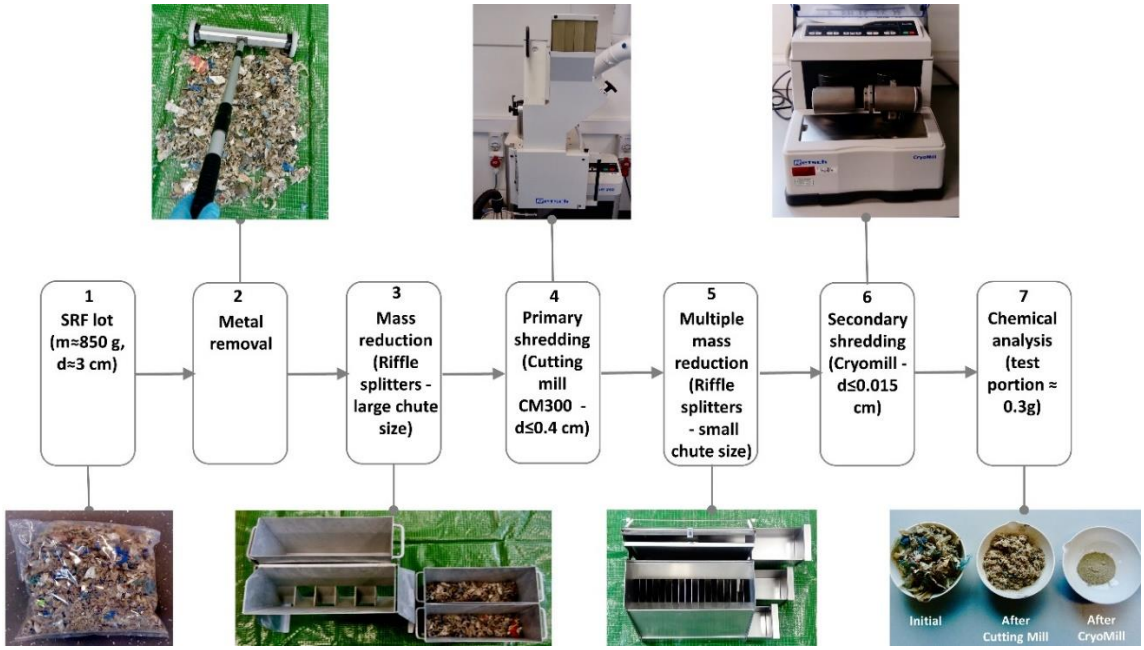

Figure 1. Sub-sampling protocol applied to SRF for quality characterization: operations and equipment were informed by best practices according to the TOS. SRF was selected an a representative solid waste-derived material with intermediate level of heterogeneity.

2.2.2 ToS-based formula

We used the theoretical model for the calculation of *fundamental error* (FE) provided by ToS. *Fundamental error* is the minimum sampling uncertainty that is attributed only to the physical and chemical constitutional heterogeneity of the sample, other factors related to sample preparation, sampling method and chemical analysis that may introduce additional uncertainty are not included (Pitard, 1993):

$$s_{FE}^2 = \left(\frac{1}{M_S} - \frac{1}{M_L}\right) Cd^3 \qquad \textbf{Eq. 2.1}$$

where M_s is the sample mass [g], M_L is the mass of the lot [g]; C is the sampling constant [g cm^{-3}]; and d is the nominal size of the particles [cm].

This formula could, also, be used in sub-sampling either for the calculation of minimum sub-sampling uncertainty (FE) for a given sample size or for the calculation of the required sample mass to obtain a specified FE (Dominy et al., 2019). At each stage of sub-sampling, M_s is the mass of the sub-sample at this stage and M_L is the mass of sample or higher level of sub-sample (Gerlach and Nocerino, 2003).

The square root of s_{FE}^2 gives the relative deviation of the FE expressed as (%). Every stage of mass splitting introduces FE, the summation of which gives the overall FE of the sub-sampling process. An overall FE ≤ 15% is a recommended acceptable reference limit (Dominy et al., 2019; Dominy et al., 2018b; Gerlach and Nocerino, 2003), although the limit value depends on the fitness for purpose requirements that are different for each application (Ramsey and Thompson, 2007).

Sampling constant, C, is the product of four factors related to the characteristics of the sample:

$$C = cflg \qquad \textbf{Eq. 2.2}$$

where c is the mineralogical (or composition) factor [g cm^{-3}]; *l* is the dimensionless liberation factor; f is the dimensionless shape factor; and g is the dimensionless particle size range (or granulometric) factor. The physical characteristics of a sample change after shredding and therefore the values of these factors (BS 15442, 2011).

The mineralogical factor, c, is defined as follows:

$$c = \lambda_M \frac{(1 - a_L)^2}{a_L} + \lambda_g (1 - a_L) \qquad \textbf{Eq. 2.3}$$

where a_L is the concentration of the critical component in the sample expressed as decimal proportion (Total [Cl] in the present study); λ_M is the density of particles containing the critical component (e.g. plastic, textile or food materials that contain Cl) [g cm^{-3}]; and λ_g is the density of the sample (SRF in the present study) [g cm^{-3}].

The factors required for the calculation of the sampling constant, C (**Eq. 2.1)** after each stage of shredding were determined as follows:

Liberation factor (l): ranges between 0 and 1 depending on the degree of heterogeneity. The more homogeneous the sample, the lower the *l* value. For the heterogeneous SRF, we selected the value 1, as the maximum value is recommended for environmental applications (Gerlach and Nocerino, 2003). After primary shredding the value was set at 0.8 (considered as *very heterogeneous material*) and after secondary shredding at 0.4 (considered *as heterogeneous material*). The selection of these values was based on the optical observation of color uniformity in SRF sub-samples after each shredding process and the guidance on the liberation parameter estimates provided by ToS (Gerlach and Nocerino, 2003).

Shape factor (f): ranges between 0 and 1 depending on closeness of particle's shape to a perfect cube (where *f* = 1.0). SRF mainly manufactured from MSW is a fluff-type material and a value of 0.05 is recommended by BS 15442 (2011). We selected the 0.2 (*soft*

homogeneous such as gold flakes) and 0.5 (*all particles are spheres such as minerals*) for the stages of primary and secondary shredding, respectively. These values were selected based on the optical observation of the particle's shape of sub-samples and on characteristic values of shape parameters for several materials given by ToS (Gerlach and Nocerino, 2003).

Granulometric factor (g): accounts for the particle size distribution (PSD) by adjusting the particle sizes to a nominal value. The more uniform the particles, the higher the g value. According to BS 15442 (2011), the *g* factor should be kept at 0.25 for PSD $d_{95}/d_{05} > 4$. Even after secondary shredding this ratio was higher than four (results presented in **Section 3.1.1**), so the factor remained constant.

Mineralogical factor (c): **Eq. 2.3** needs to define Total [Cl] of the sample and the density both of SRF and particles containing the Cl. The arithmetic mean of Total [Cl] in 16 sub-samples constituted the concentration of critical component (a_L). We considered the most prevalent chlorinated compounds in MSW for the calculation of the density of particles containing Cl in SRF (λ_M): PVC and NaCl with density 1.38 and 2.17 g cm^{-3}, respectively (Guo et al., 2001; Ma et al., 2010; PubChem, 2019). Literature findings stated that 50-75% w/w of Total [Cl] in MSW mainly attributed to the presence of plastics and 25-50% w/w mainly attributed to the presence of food waste (Gerassimidou et al., 2020). We assumed that 75% of Total [Cl] was due to PVC and 25% was due to NaCl, as the fraction of plastics in SRF can be higher than in MSW due to sorting processes applied in MT plant. The weighted average of PVC and NaCl set the λ_M value at 1.58 g cm^{-3}. The SRF density was set at 0.15 g cm^{-3} (CEN/TS 15401, 2010).

Note that the above selected values of sampling factors were used only as estimators based on ToS and SRF characteristics. The precise quantification of these factors is difficult as a significant amount of information, not available here, is required for the target material

(Ramsey and Thompson, 2007). The purpose of theoretical ToS calculations was the quantification of the effects of alternative shredding scenarios and not the precise calculation of FE.

2.2.3 Fundamental error based on three shredding scenarios

The FE was calculated based on three sample preparation scenarios: *sub-sampling without shredding (NS),* where only riffle splitting took place; *sub-sampling with only primary shredding (PS)*, where riffle splitting and only primary shredding (with cutting mill) after the first stage of riffle splitting took place; and *current sub-sampling plan (CS)*, where riffle splitting and both primary and secondary shredding, took place based on the established sub-sampling process (see **2.2.1**). Specifically, we constructed nomographs that depict the trend of s_{FE}^2 as a function of sample mass during sub-sampling for the three different shredding scenarios. The comparison amongst the different shredding scenarios enabled us to quantitatively determine the impact of shredding on the sub-sampling uncertainty based on ToS formula.

Special attention was paid to cryomill due to its effective shredding ability and confined laboratory application. We examined the effect of several configuration settings provided by the cryomill on the FE so that to select the most suitable shredding program. Specifically, four cryomill programs were selected: i) P2 with 2 grinding cycles, 2min grinding time, 1min intermediate cooling and 30 Hz grinding frequency; ii) P4 with 4 grinding cycles, 2min grinding time, 1min intermediate cooling and 30 Hz grinding frequency; iii) P5 with 5 grinding cycles, 2min grinding time, 2min intermediate cooling and 30 Hz grinding frequency; and iv) P9 P5 with 9 grinding cycles, 2min grinding time, 2.5min intermediate cooling and 25Hz grinding frequency. Common metrics of PSD, such as d_{90}, d_{50}, d_{10} and span, were used to statistically compare the shredding programs. We calculated the FE

274 introduced during: the final stage of sub-sampling from test sub-sample (7 g) to test portion
275 (0.3 g); and the entire sub-sampling from the initial sample (850 g) to test portion (overall
276 FE). The particle size of the test sub-sample was replaced by the d_{90} of each program in **Eq.**
277 **2.1**.

278 ### 2.2.4 Incorrect sub-sampling practices related to shredding

279 Despite the calculation of FE that provides the minimum uncertainty under a perfect sub-
280 sampling process, we monitored practices that may introduce bias and increase the
281 uncertainty arising from sub-sampling. Specifically, three main aspects of incorrect sub-
282 sampling practices mostly related to shredding were checked:

283 (1) Loss of sample mass by weighing individually the sub-samples after each step of sub-
284 sampling; (2) evaporation of moisture during primary and secondary shredding by obtaining
285 3 test sub-samples of 7 g with riffle splitters from a pre-dried sub-sample of 50 g and taking 6
286 replicates of residual moisture (see **2.2.6**) before and after each shredding process; and (3)
287 analytical error respecting Cl recovery by using reference materials. Synthetic mixtures with
288 known composition and consequently Total [Cl] resembling the composition of SRF were
289 prepared and analysed. Specifically, two mixtures composed of powered biomass polymers,
290 such as cellulose, xylan (common type of hemicellulose) and lignin, and plastic polymers,
291 such as HDPE, PP, PET and PVC with Total [Cl] 0.62% w/w and 1.42% w/w, respectively,
292 were prepared. The presence of Cl in the synthetic mixtures was attributed only to the
293 presence of PVC with Total [Cl] 53.7 % w/w.

294 The recovery of Cl (*R*) is given by the following equation (Prichard and Barwick, 2007):

$$R(\%) = \frac{\overline{x}}{x_0} * 100 \qquad \textbf{Eq. 2.4}$$

295 where *R (%)* is the Cl recovery, $\overline{x}$ is the mean value of Total [Cl] obtained from analysis and
296 x_0 is the assigned Total [Cl].

297 The analytical results of Total [Cl] in SRF sub-samples were corrected as shown below:

$$C_{cor} = \frac{C_{obs}}{R(\%)} * 100 \qquad \textbf{Eq. 2.5}$$

298 where C_{cor} is the corrected measurement result, C_{obs} is the observed measurement result and
299 *R(%)* is the recovery of Cl.

300 **2.2.5 Statistical analysis**

301 Analysis of variance (ANOVA) was conducted to statistically compare: the 4 different
302 cryomill programs with respect to PSD metrics; and the moisture content of sub-samples
303 before and after each shredding process (TIBCO Statistica^{TM} 13.3.0 software). The key
304 requirements to use ANOVA were checked (see **SI**).

305 Graphical illustrations were designed to assess the experimental results derived from the
306 analysis of 16 test sub-samples, in which three test portions obtained for the determination of
307 Total [Cl] and moisture content (MC) in SRF sample. Specifically, 95% confidence interval
308 error bars of mean values for each test sub-sample were designed to assess the precision of
309 analytical measurements. Additionally, boxplots were designed to provide the dispersion of
310 Total [Cl] and MC arising from the average values of test sub-samples and classify the
311 initially obtained SRF sample based on the classification scheme (BS 15359, 2011).

312 We estimated the possibility to obtain a representative test sub-sample following the
313 established sub-sampling plan for determination of Total [Cl] by calculating the confidence
314 interval for binomial proportions with three different methods (normal approximation, exact
315 Clopper-Pearson and Wilson score method). Further details can be found in the supporting
316 information (see **SI.6**). Assuming that a test sub-sample is representative if its average value

differs from the actual Total [Cl] in the initially obtained SRF sample less than 15%. We presumed that the average value of Total [Cl] from the 16 test sub-samples represents the actual Total [Cl] in the initially obtained sample.

2.2.6 Analytical techniques

Wet laser diffraction analysis was used to determine the PSD of the test sub-samples shredded by cryomill. Measurements performed by Mastersizer (2000E hydro SM, Malvern, UK) and five replicates taken for each cryomill program. The MC in SRF, expressed in % w/w, was determined according to the BS 15414-3 (2011). The residual MC is the remaining moisture after sample pre-drying at 40ºC. The total MC was calculated as follows:

$$MC_{Total} = MC_b + MC_{residual}(1 - \frac{MC_b}{100}) \qquad \textbf{Eq. 2.6}$$

The Total [Cl] in SRF measured with the standard method BC (BS 15400, 2011) and the photometric method of Palintest Chloridol test (BS 15400, 2011; Palintest-Test instructions, 2019). This photometric method uses tablets of silver nitrate that react with the chlorides of the test portion (1:50 dilution ratio) producing silver chloride. The insoluble silver chloride is observed as turbidity in the test portion measured by Palintest Photometer, which is proportional to Total [Cl]. The analytical measurements were expressed in % w/w on a dry basis (w/w_d).

3 Results and Discussion

3.1 Beneficial effects of shredding based on ToS

3.1.1 Effect of cryomill settings on fundamental error

337 **Figure 2** shows that shredding programs achieved similar PSD except for P2. Specifically,
338 d_{90} of P4, P5 and P9 ranges between 110-152 µm, and it is more than twice larger for P2 (356
339 µm) (see **SI.1**). ANOVA test showed statistical difference amongst the cryomill programs
340 regarding all PSD metrics (d_{10}, d_{50}, d_{90} and span) (see **SI.1**).

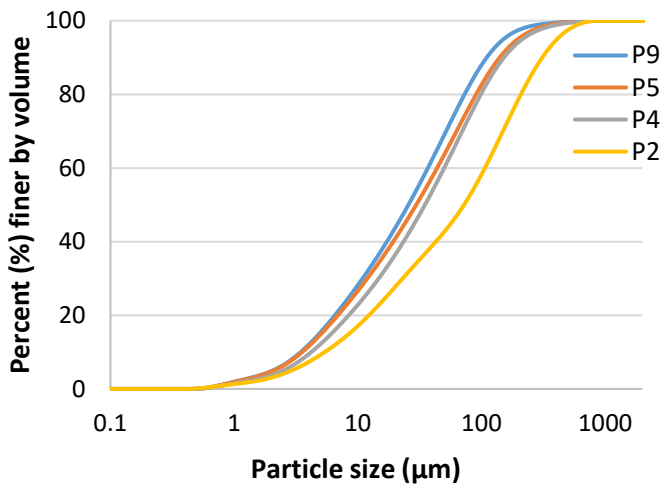

341

342 **Figure 2.** Cumulative PSD for SRF particles shredded by cryomill under 4 different
343 shredding programs.

344 However, the theoretical model of ToS (**Eq. 2.1**) showed that configuration settings of
345 cryomill do not considerably affect the overall sub-sampling uncertainty (**Figure 3**). We
346 found that the overall FE is identical for P9, P5 and P4 (33.6%), whereas for P2 a negligible
347 rise is observed (33.8%). Considerable difference can be found only in the FE arising from
348 the final stage of sub-sampling, from test sub-sample (7 g) to test portion (0.3 g). The highest
349 difference is between P9 (0.3%) and P2 (3.2%), where the FE increases more than ten times
350 at the final sub-sampling stage.

351 From the statistical point of view, the PSD is significantly different amongst the shredding
352 programs. However, this difference (µm-scale) is negligible compared to the difference (cm-
353 scale) between the particle size before (3 cm) and after (0.4 cm) primary shredding. The FE
354 of the final sub-sampling stage is considerably lower than the FE of previous stages, where

355 the particle size is one order of magnitude greater. For example, in the most extended
356 shredding program (P9) the FE arising from the final stage (0.3%) constitutes less than 1% of
357 the overall FE (33.6%). Even in the least extended program (P2) the final stage constitutes
358 less than 10% of the overall FE. We selected P4, as it was the best combination of sample
359 homogeneity (low FE), cost and time savings.

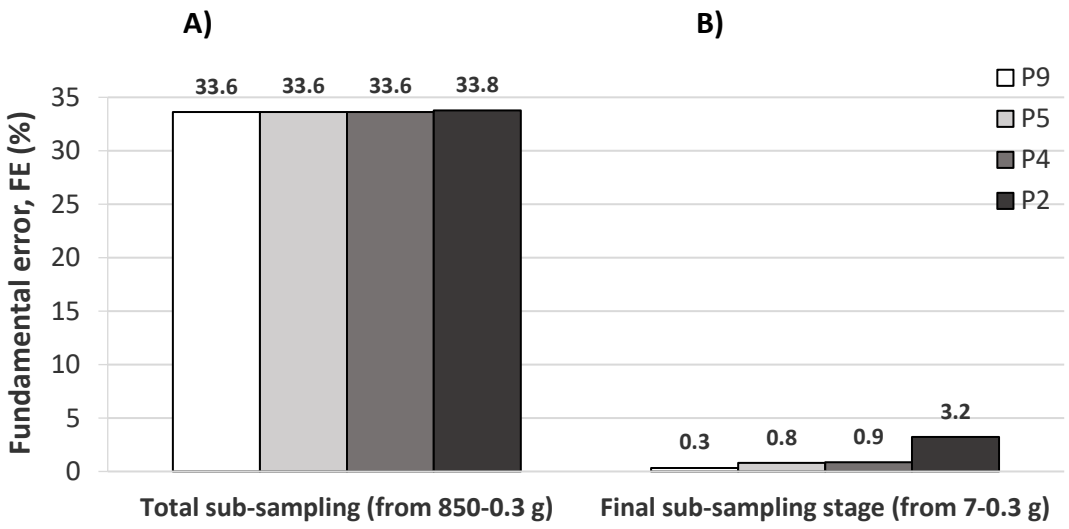

360 **Figure 3.** Fundamental error (FE) arising from the sub-sampling plan applied for the
361 determination of Total [Cl] in SRF after shredding of test sub-samples with cryomill
362 (secondary shredding) under four different configuration settings based on ToS: overall FE
363 during sub-sampling from the sample (850 g) to test portion (0.3 g) (**A**); and FE during the
364 final stage of sub-sampling from the test sub-sample (7 g) to test portion (**B**).

365 **3.1.2 Trend of fundamental error under different shredding scenarios: Nomographs**

366 Nomographs constructed for the three different shredding scenarios: sub-sampling without
367 shredding (NS), sub-sampling with primary shredding (PS), and current sub-sampling plan
368 (CS) (**Figure 4).** The points of nomographs (A to H) indicate the alteration of mass and
369 particle size of sub-samples during sub-sampling based on the three scenarios. The movement
370 from one point to another indicates the stages of shredding and riffle splitting. For example,
371 the sample was split into two sub-samples from point A to B (from 850 g to 425 g), the sub-
372 samples were shredded with the cutting mill (primary shredding) from point B to D,

consecutive stages of riffle splitting took place from point D to E, and so on.

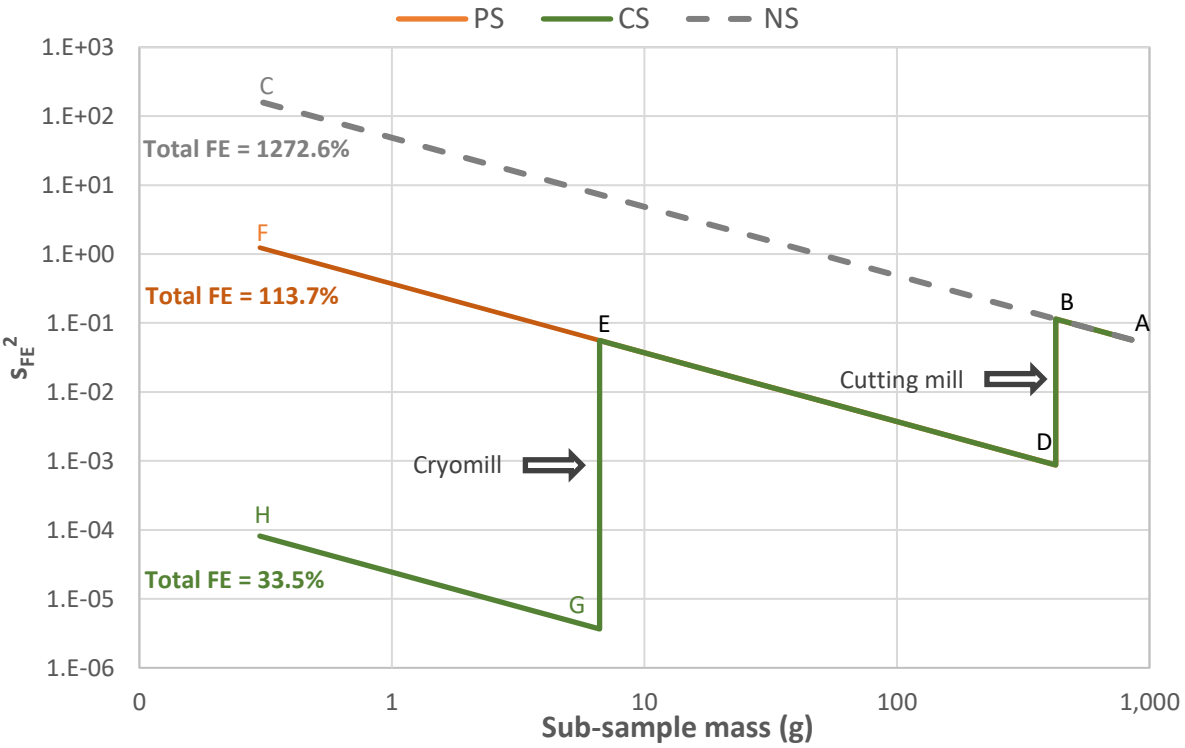

Figure 4. Trend of the variance of fundamental error (s_{FE}^2) during sub-sampling (nomograph) for the determination of Total [Cl] in SRF under three shredding scenarios: **NS** -sub-sampling without shredding (A-B-C); **PS** - sub-sampling with primary shredding (A-B-D-E-F); **CS** - the current sub-sampling plan including both primary and secondary shredding (A-B- D-E-G-H). The points above the trend lines demonstrate the mass and the particle size alteration of sub-samples during sub-sampling. The movement from one point to another indicate the stages of sub-sampling.

For the three scenarios the process from point A to B is identical as shredding took place after the first stage of rifle splitting, while scenarios PS (points A-B-D-E-F) and CS (points A-B-D-E-G-H) are identical from point A (from sample of 850 g) to D (test sub-sample of ca. 7 g) as secondary shredding applied after the obtainment of the test sub-sample. For these two scenarios (PS and CS), the 1st stage of riffle splitting (from A to B) applied before primary shredding introduces the highest uncertainty (FE: 23.9%) compared to the next sub-sampling

stages due to the largest particle size (d ≈ 3 cm). This phenomenon indicates the urgent need for primary shredding, which drops the FE in the next stages of rifle splitting.

If no primary shredding applied, which is the NS scenario (A-B-C), the uncertainty would be increased logarithmically during sub-sampling (overall FE: 1272.6%). The considerably lower uncertainty observed in the PS scenario (overall FE: 113.7%) indicates that primary shredding applied after the 1st stage of riffle splitting can reduce the overall FE more than 11 times. By comparing the PS with the CS scenario (overall FE: 33.5%), the overall FE decreases more than 3 times if the particle size of the test sub-sample drops from 0.4 cm to 0.015 cm. The beneficial role of cryomill is also revealed by the contribution of the final stage of sub-sampling to the overall FE for the two scenarios: *PS* and *CS*. For the PS scenario, the FE arising from the final stage of sub-sampling (FE from E to F: 108.7%) contributes 96% to the overall FE, whereas the FE arising from the final stage for the CS scenario (FE from G to H: 0.9%) contributes less than 3% to the overall FE. Note that these differences do not include any bias that might be induced by a larger particle size (e.g., insufficient Cl recovery). The calculations conducted for the construction of nomograph (**Figure 4**) and the estimation of FE arising from each sub-sampling stage is presented in **SI.2.**

3.2 Adverse effects of shredding: *incorrect* sampling practices

3.2.1 Moisture evaporation during shredding

The moisture evaporation during shredding may lead to the miscalculation of residual MC and therefore of Total [Cl] expressed on a dry basis. Based on the ANOVA test, we cannot reject the null hypothesis that shredding processes (primary and secondary) do not affect the

411 MC (see **SI.3**). Similarly,

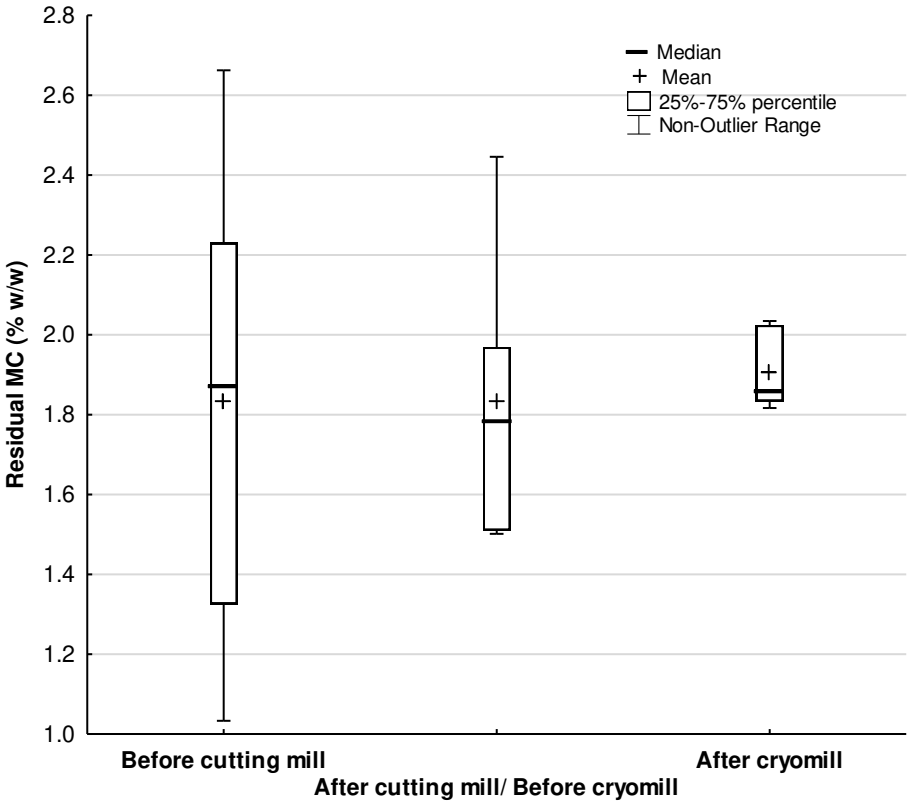

412

413 **Figure 5** shows that residual MC is not affected by the shredding processes, although a

414 negligible decrease after primary shredding with cutting mill is observed. There is a slight

415 increase in residual MC after secondary shredding (cryomill). These insignificant differences

416 of residual MC amongst the shredding stages can be attributed to SRF inherent heterogeneity.

417 The test sub-samples for each shredding stage were drawn from the same sub-sample, but

418 they were not identical.

419

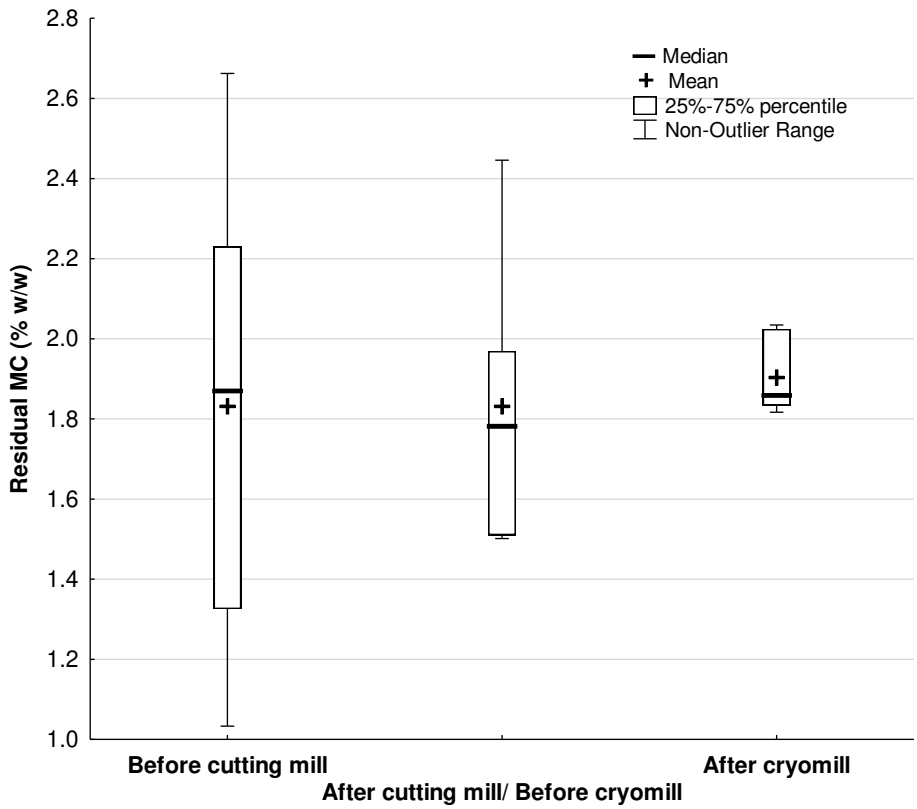

Figure 5. Residual MC in test sub-samples obtained by an SRF sub-sample of 50 g before and after two shredding processes: primary with the use of cutting mill and secondary with the use of cryomill.

3.2.2 Loss of sample mass during sub-sampling

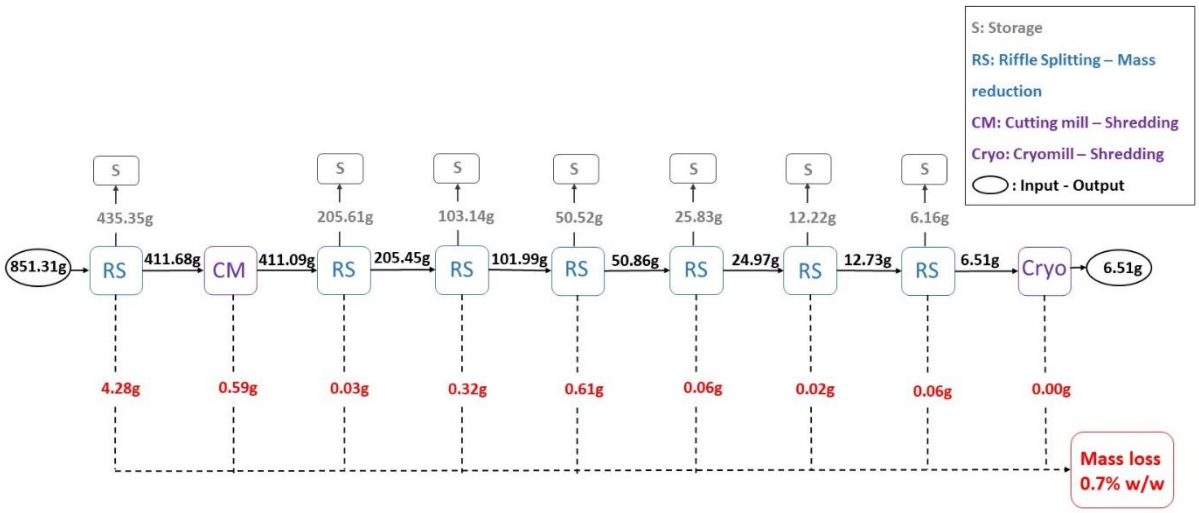

Figure 6 shows the loss of sample mass induced at each stage of the sub-sampling process (riffle splitting and shredding). We found that the mass loss cannot be zero, even under

careful sub-sampling practices conducted by a well-trained operator. It should be noted that riffle splitters are composite sub-sampling devices with high performance depending on the training skills of operator and the fraction of fines in the sample (Gerlach and Nocerino, 2003). The loss of sample mass is 0.7% w/w mainly due to the considerable fraction of fines in SRF. The first stage of riffle splitting, that took place before primary shredding, induced 72% of the total mass loss (4.28 g out of 5.97 g) during the sub-sampling. At this stage of mass splitting, the range of particle size and the sample mass are maximum making sample handling more difficult. Primary shredding contributes nearly 10% to the total mass loss which corresponds to 0.07% w/w of total sample mass, whereas no loss occurs during secondary shredding. Although 5.97 g out of 851.31 g had zero probability to be included in the test portion for analysis violating the fundamental principle of ToS, this amount can be considered negligible (Edjabou et al., 2015).

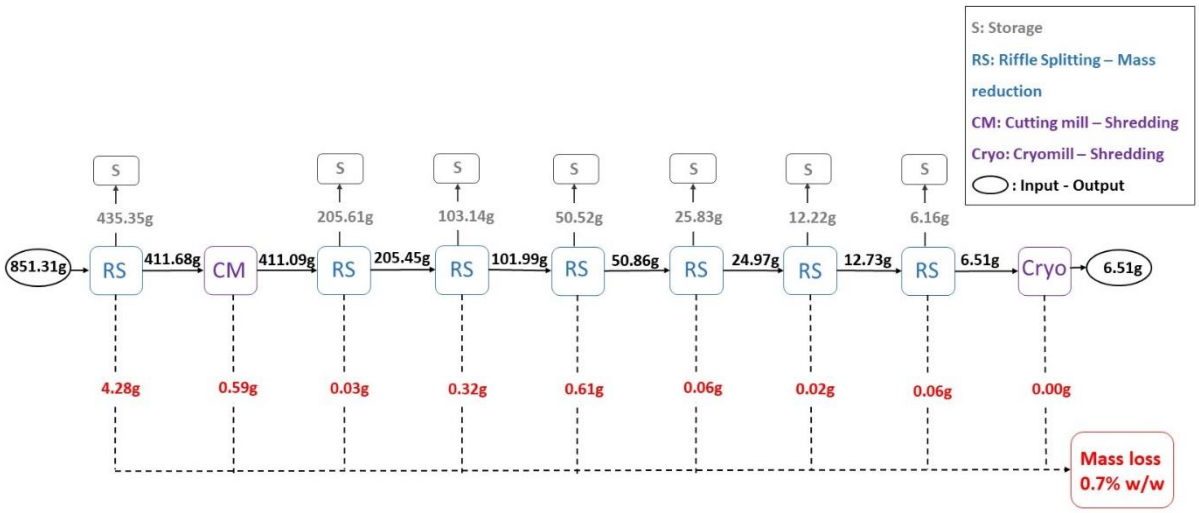

Figure 6. Mass flow analysis of SRF sample (ca. 0.85 kg), expressed in grams, during the sub-sampling process that consists of consecutive steps of mass reduction (riffle splitting) and two shredding stages (by using cutting mill and cryomill) for the obtainment of a test sub-sample (ca. 7 g).

3.2.3 Recovery of Cl from cryogenically shredded sub-samples

447 The recovery (*R*) of Total [Cl] from synthetic mixtures account for a range between 98.0 to
448 98.6% (**Table 1**). Even cryogenic shredding of synthetic mixtures did not reach 100% *R* of
449 Total [Cl]. Cuperus et al. (2005) estimated the *R* of the Total [Cl] in SRF by means of BC
450 combined with ion chromatography (IC), reporting that *R* can reach up to 100% when the
451 particle size of the test portion is < 5 mm. Here, the size is lower (0.15 mm), but *R* is not
452 100%. Hence, the reason might be the loss of Cl during the bomb ventilation. Ma et al.
453 (2010) reported that BC measures less Total [Cl] compared to other analytical methods due to
454 potential incomplete combustion in the bomb or Cl loss during bomb ventilation. The
455 analytical values of Total [Cl] in SRF sub-samples were corrected based on **Eq. 2.5** by taking
456 the average of the recoveries from both synthetic mixtures.

457 **Table 1.** Recovery of Total [Cl] from synthetic mixtures with assigned Total [Cl] resembling
458 SRF composition using BC – Palintest Chloridol analytical method.

SRF components	**Synthetic SRF 1**			**Synthetic SRF 2**		
	Composition (% w/w)[1]	Assigned Total [Cl] (% w/w)	Observed Total [Cl] (% w/w)[2]	Composition (% w/w)[1]	Assigned Total [Cl] (% w/w)	Observed Total [Cl] (% w/w)[2]
Cellulose	33.81	0		34.33	0	
Xylan	4.02	0		4.05	0	
Lignin	17.08	0		15.02	0	
HDPE	14.70	0		15.02	0	
PP	22.14	0		21.32	0	
PET	7.11	0		7.63	0	
PVC	1.15	53.71		2.64	53.71	
Total	**100**	**0.62**	**0.61**	**100**	**1.42**	**1.39**
Recovery (%)[3]			**98.58**			**98.03**

[1]The composition of the mixtures was based on literature evidences (Cuperus et al., 2005; Heikkinen et al., 2004); [2]The value derived from the arithmetic mean of three replicates; [3]**Eq. 2.4**.

459 **3.3 Fitness for purpose of sub-sampling plan: Representativeness of test sub-samples**

Figure 7 shows the measurement precision (95% confidence interval error bars of mean values from each measurement) and the dispersion (boxplots) of the 16 test sub-samples obtained for the determination of Total [Cl] and MC. The dotted red lines indicate the arithmetic mean of Total [Cl] (1.08% w/w_d) and MC (16.7% w/w) derived from the 16 test sub-samples. **Figure 7** provides an overview for the risk to obtain non-representative results for the determination of SRF properties with higher (e.g. Cl) or lower (e.g. moisture) variability.

Assuming that the average values of 16 measurements represent the actual Total [Cl] and MC in the initially obtained SRF sample, then the potential to over- or under-estimate the critical component in the sample is present by drawing one test sub-sample. For example, the selection of the 4th sub-sample with the highest Total [Cl] (1.38 % w/w_d) would overestimate the Total [Cl] in the sample (1.08% w/w_d) by 27.6%, whereas the 14th sub-sample with the lowest value (0.90% w/w_d) would underestimate the Total [Cl] by 16.4%. However, the majority of the test sub-samples does not differ from the mean value more than 15% except from the 7th (19.9% overestimation), the 4th (27.6% overestimation) and 14th (16.4% underestimation) sub-samples (see **SI.4**).

The difference between the minimum and maximum value leads to a range of 0.48% w/w_d, which is equal with a relative range 44%. This range is comparable with the intervals between the class codes for the limit values of Cl content in SRF specified by the European Committee of Standardization (CEN) classification scheme (BS 15359, 2011). For example, the difference of Total [Cl] between class code 2 (≤ 0.6% w/w_d) and class code 3 (≤ 1% w/w_d) is 0.4% w/w_d which is lower than the range of Total [Cl] in the 16 test sub-samples, whereas the difference between class code 3 (≤ 1% w/w_d) and class code 4 (≤ 1.5% w/w_d) is slightly higher (0.5% w/w_d).

The determination of Total [Cl] in the 16 sub-samples leads to different classification results amongst the SRF sub-samples: 7 out of 16 sub-samples are designated as class code 3 and 9 out of 16 sub-samples are designated as class code 4 (**Figure 7**). The different classification amongst the 16 sub-samples is mainly due to the proximity of mean value (1.08% w/w_d) in the border between the class code 3 and class code 4 (1.0% w/w_d).

A)

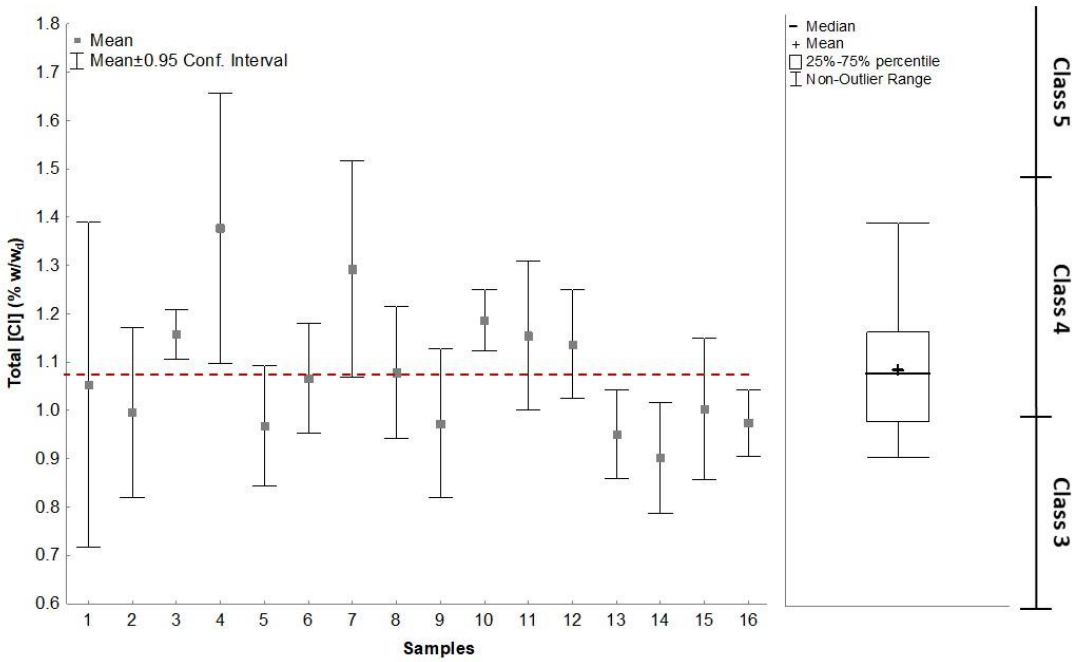

B)

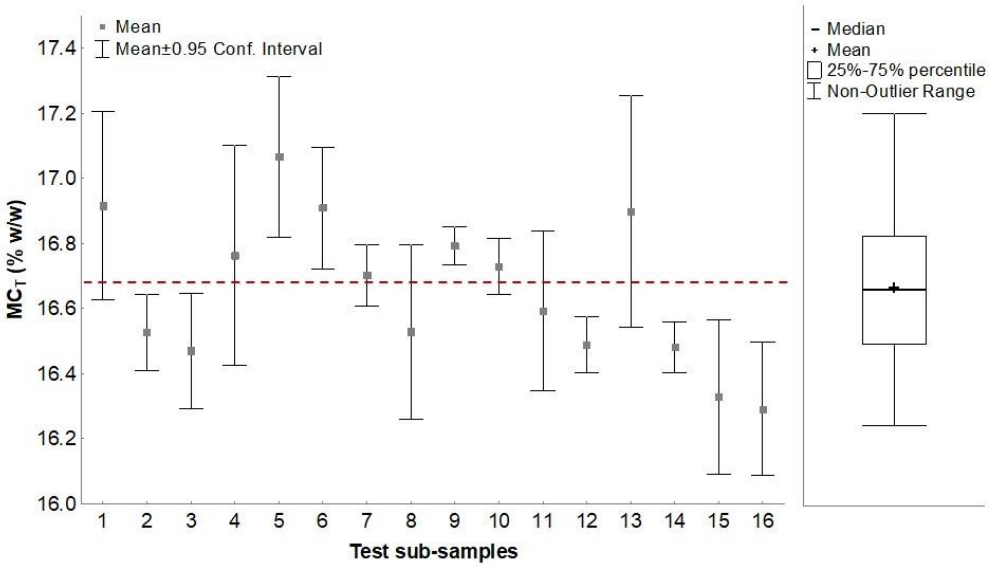

Figure 7. Variability of (**A**) Total [Cl] and (**B**) total MC (MC_T) in SRF sample delivered to the laboratory for analysis as calculated by the obtainment of 16 test sub-samples through the established sub-sampling protocol.

In the case of MC, test sub-samples are more representative. For example, the 5th sub-sample with the highest MC (17.1% w/w) would overestimate the MC in the sample by 2.5%, whereas the 16th sub-sample with the lowest MC (16.3% w/w) would underestimate the MC by 2.2%. The difference between these values leads to a range of 0.8% w/w, which is equal with a relative range of 4.6%.

The interval estimations for binomial proportion showed that the total number of representative SRF test sub-sample lies between 57 to 93% of total population with 95% confidence following the current sub-sampling plan (see **SI.5**). Therefore, the possibility to obtain a non-representative test sub-sample for the determination of Total [Cl] is not negligible. However, this possibility can be considerably reduced if we obtain and analyse two test sub-samples instead. By averaging the analytical results of two test sub-samples (see **SI.4**), we found only 5 pairs out of 120 that were non-representative for the determination of

Total [Cl]. Specifically, the total number of representative pairs of test sub-samples lies between 91 to 98% of total population with 95% confidence (see **SI.5**).

The properties of SRF should be expressed as intervals and not as individual values due to high constitutional heterogeneity so that to address the quality assurance in analytical characterization of solid waste (Chen et al., 2016; Flamme and Ceiping, 2014; Velis et al., 2010). After the chemical analysis of 16 test sub-samples, Total [Cl] in the SRF sample lies within a range of 1.01-1.15% w/w_d and the MC within a range of 16.5-16.8% w/w with 95% confidence.

4 Conclusions

First, by comparing three different sample preparation scenarios through ToS nomographs, the beneficial role of shredding in the representativeness of test sub-samples for Total [Cl] determination in SRF was quantified. Primary shredding ($d_{90} \leq 0.4$ cm) applied after the first stage of mass splitting resulted in the reduction of sub-sampling uncertainty, expressed as FE, more than 11 times compared to a non-shredded test sub-sample. The cryogenic, final shredding stage ($d_{90} \leq 0.15$ mm) applied to the test sub-sample reduced the uncertainty more than 3 times compared to primary shredding scenario. The significant contribution of cryogenic shredding to the reduction of sub-sampling uncertainty is attributed to the logarithmic increase of uncertainty as the sample mass decreases based on ToS. Therefore, we here establish that it is a highly recommended sample preparation process step for chemical analysis of waste-derived materials featuring high inherent heterogeneity. The configuration settings of cryomill had a negligible effect on the decrease of the overall uncertainty; therefore, it is feasible to identify an affordable set of operation settings for the

527 cryogenic shredding, for example with low number of grinding cycles, reducing processing
528 time and liquid nitrogen consumables cost.

529 Second, practices related to shredding that could introduce bias were assessed as negligible
530 with careful execution of the suggested sub-sampling plan. Specifically, potentially incorrect
531 sub-sampling practices were demonstrated here to be minimised: (1) shredding did not affect
532 the MC, assuring the validity of analyte determination on a dry reporting basis; (2) the loss of
533 sample mass was negligible (0.7% w/w) – but, the operator's experience is crucial and mass
534 loss could be higher if attention is not paid to best practice; and (3) the recovery of Total [Cl]
535 from cryogenically shredded test portions of artificial SRF comprising a mixture of reference
536 materials reached 98.3% - an acceptable level of analytical error.

537 Third, experimental results showed that the established sub-sampling plan lead to
538 representative analytical results related to the determination of MC (relative range < 4.6%),
539 an analyte with relatively low variability. However, in the case of Total [Cl], obtaining one
540 test sub-sample entails the risk of incorrect classification of SRF. Less than 20% of total
541 population of test sub-samples were not representative, assessed as exceeding the 15% upper
542 limit suggested by the literature. However, the selection of this limit value is arbitrary as
543 there is no relevant comparative evidence in the solid waste management sector. The
544 possibility of obtaining a non-representative test sub-sample under the current sub-sampling
545 plan lies between 7 - 43% (95% confidence), whereas drawing and averaging two test sub-
546 samples instead, considerably reduces that risk (2 - 9% with 95% confidence). However, the
547 cost and time of sub-sampling and analysis would be respectively increased.

548 Experimental results showed that the established sub-sampling plan can result in
549 representative sub-samples (13 out of 16) with uncertainty less than 15%, whereas the
550 maximum overestimation observed in the 4th test sub-sample (27.6%) did not exceed the

theoretical ToS calculations (FE: 33.5%). These findings support the need for exploring the suitability of the ToS-based formula applied for the determination of analytes with considerably variable concentrations amongst the particles/components of waste-derived materials.

The current sub-sampling scheme was conducted by using and adhering to optimal, yet practicable and affordable sampling practices and equipment, which is verified by the ability of such laboratory set up and operational regime to render satisfactory measurements. Therefore, the suggested sub-sampling plan can be used as a fitness for purpose approach to minimise potential bias, and could be incorporated in the relevant SRF sample preparation standards (BS 15413, 2011; BS 15443, 2011). To this, a round robin verification test would be needed.

Acknowledgements

We are grateful to the lab technician personnel at the Solid Waste Management and Sample Preparation laboratory at the University of Leeds, for training and generic quality assurance support.

Funding

This research did not receive any specific grant from funding agencies in the public, commercial, or not-for-profit sectors. Doctoral researcher S. Gerassimidou was funded by the University of Leeds Scholarships programme.

REFERENCES

BS 15359, 2011. Solid recovered fuels. Specifications and classes. British Standard Institution.

BS 15400, 2011. Solid recovered fuels. Determination of calorific value. British Standards Institution.

BS 15413, 2011. Solid recovered fuels. Methods for the preparation of the test sample from the laboratory sample. British Standards Institution.

BS 15414-3, 2011. Solid recovered fuels. Determination of moisture content using the oven dry method. Moisture in general analysis sample. British Standards Institution.

BS 15442, 2011. Solid recovered fuels. Methods for sampling. British Standards Institution.

BS 15443, 2011. Solid recovered fuels. Methods for the preparation of the laboratory sample. British Standards Institution.

CEN/TS 15401, 2010. Solid recovered fuels. Determination of bulk density. British Standards Institute.

Chen X., Huang G., Zhu H., Suo M. and Dong C., 2016. Inexact inventory theory–based waste management planning model for the City of Xiamen, China. *J. Environ. Eng* 142(5): 04016013.

Cheng G., Huang G., Dong C., Xu Y., Chen X. and Chen J., 2017. Distributed mixed-integer fuzzy hierarchical programming for municipal solid waste management. Part I: System identification and methodology development. *Environ. Sci. Pollut. Res.* 24(8): 7236-7252.

Cuperus J., Van Dijk E. and De Boer R., 2005. Pre-normative research on SRF. TAUW, Deventer, Netherlands, 128. Available from: http://erfo.info/fileadmin/user_upload/erfo/documents/standardisation/Final_report_Prenormative_research_on_solid_recovered_fuel.pdf (accessed 10 January 2020).

Dominy S.C., Glass H.J., O'Connor L., Lam C.K. and Purevgerel S., 2019. Integrating the Theory of Sampling into underground mine grade control strategies: case studies from gold operations. *Minerals* 9(4): 238.

Dominy S.C., Glass H.J., O'Connor L., Lam C.K., Purevgerel S. and Minnitt R.C., 2018a. Integrating the Theory of Sampling into underground mine grade control strategies. *Minerals* 8(6): 232.

Dominy S.C., O'Connor L., Glass H.J., Purevgerel S. and Xie Y., 2018b. Towards representative metallurgical sampling and gold recovery testwork programmes. *Minerals* 8(5): 193.

Edjabou M.E., Jensen M.B., Götze R., Pivnenko K., Petersen C., Scheutz C. and Astrup T.F., 2015. Municipal solid waste composition: Sampling methodology, statistical analyses, and case study evaluation. *J. Waste Manag.* 36 12-23.

Esbensen K.H. and Velis C., 2016. Transition to circular economy requires reliable statistical quantification and control of uncertainty and variability in waste. *Waste Manag. Res.* 34(12): 1197-1200.

Flamme S. and Ceiping J., 2014. Quality assurance of solid recovered fuels (SRF). *ZKG International* 67(5): 54-57.

Gerassimidou S., Velis C.A., Williams P.T., Castaldi M.J., Black L. and Komilis D., 2020. Chlorine in waste-derived solid recovered fuel (SRF), co-combusted in cement kilns: A systematic review of sources, reactions, fate and implications. *Crit. Rev. Env. Sci. Tec.* 1-47.

Gerlach R.W., Dobb D.E., Raab G.A. and Nocerino J.M., 2002. Gy sampling theory in environmental studies. 1. Assessing soil splitting protocols. *J. Chemom.* 16(7): 321-328.

Gerlach R.W. and Nocerino J.M., 2003. Guidance for obtaining representative laboratory analytical subsamples from particulate laboratory samples. Environmental Protection Agency, USA, Available from: https://nepis.epa.gov/Exe/ZyNET.exe/2000GTWM.TXT?ZyActionD=ZyDocument&Client=EPA&Index=2000+Thru+2005&Docs=&Query=&Time=&EndTime=&SearchMethod=1&TocRestrict=n&Toc=&TocEntry=&QField=&QFieldYear=&QFieldMonth=&QFieldDay=&IntQFieldOp=0&ExtQFieldOp=0&XmlQuery=&File=D%3A%5Czyfiles%5CIndex%20Data%5C00thru05%5CTxt%5C00000009%5C2000GTWM.txt&User=ANONYMOUS&Password=anonymous&SortMethod=h%7C-&MaximumDocuments=1&FuzzyDegree=0&ImageQuality=r75g8/r75g8/x150y150g16/i425&Display=hpfr&DefSeekPage=x&SearchBack=ZyActionL&Back=ZyActionS&BackDesc=

630 Results%20page&MaximumPages=1&ZyEntry=1&SeekPage=x&ZyPURL (accessed 20
631 January 2020).

632 Glass G.V. and Hopkins K., 1996. *Statistical methods in psychology and education.* 3rd ed.
633 Allyn & Bacon, Boston, USA.

634 Guo X.-f., Yang X.-l., Li H., Wu C.-z., Chen Y., Li F. and Xie K.-C., 2001. Release of
635 hydrogen chloride from combustibles in municipal solid waste. *Environ. Sci. Technol.*
636 35(10): 2001-2005.

637 Gy P., 2012. *Sampling of particulate materials theory and practice.* Elsevier, Netherlands

638 Harwell M.R., Rubinstein E.N., Hayes W.S. and Olds C.C., 1992. Summarizing Monte Carlo
639 Results in Methodological Research: The One- and Two-Factor Fixed Effects ANOVA
640 Cases. *J. Educ. Stat.* 17(4): 315-339.

641 Heikkinen J., Hordijk J., de Jong W. and Spliethoff H., 2004. Thermogravimetry as a tool to
642 classify waste components to be used for energy generation. *J. Anal. Appl. Pyrol.* 71(2): 883-
643 900.

644 Iacovidou E., Hahladakis J., Deans I., Velis C. and Purnell P., 2018. Technical properties of
645 biomass and solid recovered fuel (SRF) co-fired with coal: impact on multi-dimensional
646 resource recovery value. *J. Waste Manag.* 73: 535-545.

647 Junghare H., Hamjade M., Patil C., Girase S. and Lele M., 2017. A Review on Cryogenic
648 Grinding. *Int. J. Curr. Eng. Technol.* Special Issue - 7.

649 Kallassy M., Efremenko B. and Champel M., 2008. Waste processing: the status of
650 mechanical and biological treatment. ISWA Beacon conference "The global challenge:
651 optimising the cycle of biuological treatment of biowaste", Perugia, Italy.

652 Ma W., Hoffmann G., Schirmer M., Chen G. and Rotter V.S., 2010. Chlorine characterization
653 and thermal behavior in MSW and RDF. *J. Hazard. Mater.* 178(1-3): 489-498.

654 Montgomery D.C., 2017. *Design and analysis of experiments.* John Wiley & Sons, New
655 York, USA.

656 Nocerino J.M., Schumacher B.A. and Dary C.C., 2005. Role of laboratory sampling devices
657 and laboratory subsampling methods in representative sampling strategies. *Environ.*
658 *Forensics* 6(1): 35-44.

Palintest-Test instructions, 2019. Chloride (Chloridol)-Photometer method. Available from https://www.palintest.com/wp-content/uploads/2019/04/Phot.46.AUTO-Chloride-Chloridol-v3.pdf (accessed 24 April 2019).

Pitard F.F., 1993. *Pierre Gy's sampling theory and sampling practice: heterogeneity, sampling correctness, and statistical process control.* CRC press, Florida, USA.

Prichard E. and Barwick V., 2007. *Quality assurance in analytical chemistry.* John Wiley & Sons, Teddington, UK.

PubChem, 2019. Sodium chloride. National Center for Biotechnology Information. Available from https://pubchem.ncbi.nlm.nih.gov/compound/sodium_chloride (accessed 10 May 2019).

Ramsey M.H. and Thompson M., 2007. Uncertainty from sampling, in the context of fitness for purpose. *Accredit. Qual. Assur.* 12(10): 503-513.

Retsch, 2011. Sample preparation & quality control. Available from http://www.macrolab.com.ua/pdf/brochure_general_en.pdf (accessed 11 June 2019).

Retsch, 2020a. Cryomill. Available from https://www.retsch.com/products/milling/ball-mills/mixer-mill-cryomill/function-features/ (accessed 11 June 2020).

Retsch, 2020b. Cutting Mill SM 300. Available from https://www.retsch.com/products/milling/cutting-mills/sm-300/function-features/?gclid=Cj0KCQjww_f2BRC-ARIsAP3zarEvhShkjkmqKH9QQHKKFh7EC5dKeVmKlFDnhk1YgAegeDvFFEoR_msaAvxUEALw_wcB (accessed 11 June 2020).

Velis C., Longhurst P.J., Drew G.H., Smith R. and Pollard S.J., 2010. Production and quality assurance of solid recovered fuels using mechanical—biological treatment (MBT) of waste: a comprehensive assessment. *Crit. Rev. Env. Sci. Tec.* 40(12): 979-1105.